OPEN ACCESS
Journal of Multidisciplinary Applied Natural Science Vol. xx No. xx (xxxx) https://doi.org/10.47352/jmans.2774-3047.365
Check for updates
Research Article

Furosemide Increases $GABA_A$ Receptor Activity via Antagonism to Sodium-Potassium-Chloride Cotransporter 1 *In Silico* and *In Vivo*

Marsintauli Hasudungan Siregar*, Nurdiana Nurdiana, Farhad Bal'afif, Susanthy Djajalaksana, and Arif Setiawansyah

Received : August 2, 2025	Revised : November 20, 2025	Accepted : December 4, 2025	Online : March 5, 2026

Abstract
GABAA receptor dysfunction and altered chloride homeostasis significantly contribute to seizure pathophysiology, with the sodium-potassium-chloride cotransporter 1 (NKCC1) playing a crucial role in regulating neuronal excitability. This study investigated furosemide's capacity to enhance GABAA receptor activity through NKCC1 antagonism and evaluated its therapeutic profile in combination with diazepam for seizure management. Comprehensive molecular docking analyses were conducted to assess binding affinities of furosemide and diazepam to NKCC1, followed by *in vivo* experiments using pentylenetetrazol-induced seizure models to evaluate GABAA receptor expression, seizure duration, and multiple pathophysiological biomarkers. Molecular analysis revealed that furosemide demonstrated measurable NKCC1 binding capacity (binding energy: -7.09 kcal/mol; Ki: 6.34 µM), though significantly lower affinity compared to diazepam (binding energy: -7.83 kcal/mol; Ki: 1.81 µM). The furosemide-diazepam combination exhibited complex competitive binding interactions, with furosemide substantially reducing diazepam's NKCC1 binding affinity. NKCC1 antagonism by furosemide effectively enhanced GABAA receptor expression by 29.8 ± 1.60% when used alone and 37.60 ± 2.0% in combination with diazepam. However, combination therapies resulted in significantly longer seizure durations (80 ± 3.0 s) compared to diazepam monotherapy (42.5 ± 2.10 s), suggesting antagonistic interactions on acute seizure suppression that may reflect altered chloride gradients or competitive pharmacokinetic effects. Despite reduced efficacy in seizure termination, combination therapy demonstrated selective advantages in other pathophysiological domains, including superior blood-brain barrier protection (reduced albumin level to 90.90 ± 2.70 µg/mL) and reduced excitotoxic damage. These findings indicate that furosemide-diazepam combination therapy presents a complex therapeutic profile characterized by trade-offs between acute seizure control and neuroprotective mechanisms. The data suggest potential utility in maintenance therapy or prevention of seizure-related complications rather than acute seizure termination, warranting further investigation into temporal optimization strategies and dose modifications.

Keywords: anticonvulsant, combination therapy, diazepam, furosemide, GABAergic, NKCC1 antagonism

1. INTRODUCTION

Status epilepticus (SE) is clinically defined as continuous epileptiform activity or seizures lasting more than 5 min [1]. SE progresses rapidly through several stages, starting with discrete overmotor seizures, subclinical electrographic seizures, and persistent seizures that remain refractory and self-sustaining due to a lack of responsiveness to pharmacological treatment. In this model, seizures are induced by administering pentylenetetrazole (PTZ), which inhibits the binding of gamma-aminobutyric acid (GABA) to its receptors. These seizures result in widespread apoptotic neuronal cell death, particularly in regions such as the hippocampus. This model is considered a valid representation of human generalized myoclonic and absence seizures [2][3].

The first-line treatment for SE is diazepam, a benzodiazepine (BZD) that enhances GABA-ergic activity and has demonstrated protective effects against PTZ-induced seizures [4]. Approximately 80% of seizures are effectively stopped when the first-line treatment is administered within 30 min; however, prolonged treatment is associated with a poorer prognosis and an increased risk of chronic adverse effects. SE initially responds to BZD treatment within 2 min, but the response rate drops to less than 50% if treatment is delayed by 15–30 min. This highlights the importance of prompt intervention to minimize the risk of treatment resistance [5].

Both clinical and animal studies highlight a rapid loss of diazepam's potency as seizures persist, resulting in diminished synaptic inhibition and the onset of self-sustained seizures. Consequently, up to 40% of SE cases fail to respond to BZD treatment

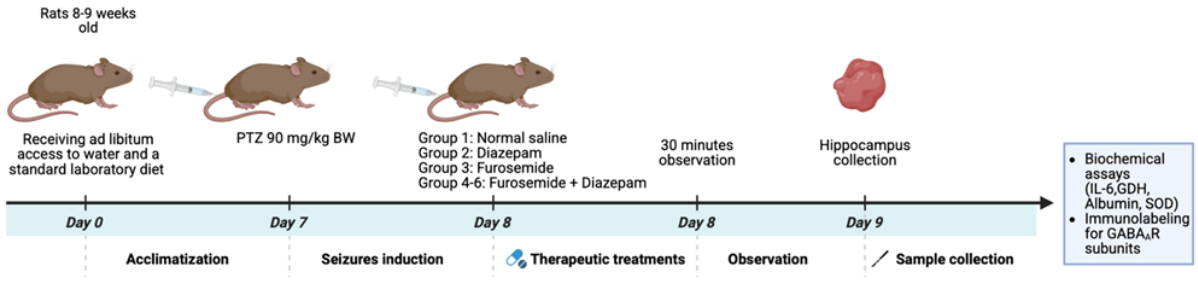

Figure 1. The *in vivo* experimental workflow.

[5]. The development of pharmacoresistance in SE is thought to stem from a reduction in BZD-sensitive GABA-ergic inhibition [6]-[8]. Current understanding suggests that pharmacoresistant SE results from pathological alterations in chloride homeostasis, which compromise GABA-ergic inhibition [9][10]. Effective GABA-ergic inhibition and BZD modulation require the maintenance of low intracellular chloride levels through the coordinated function of chloride transporters, particularly the sodium-potassium-chloride cotransporter 1 (NKCC1) and the potassium-chloride cotransporter 2 (KCC2) [11][12].

Recent advances in understanding the molecular mechanisms underlying SE have identified disrupted chloride homeostasis as a critical factor in treatment resistance. The current therapeutic approach relies heavily on BZDs, which face significant limitations in prolonged seizure states due to receptor internalization and altered chloride gradients [13]. While second-line treatments including phenytoin, valproate, and levetiracetam exist, treatment failures remain substantial, particularly in refractory cases where traditional GABA-ergic enhancement strategies lose efficacy. The role of cation-chloride cotransporters in maintaining proper neuronal chloride homeostasis has emerged as a promising therapeutic target. NKCC1, which facilitates chloride influx, becomes pathologically upregulated during seizures, while KCC2, responsible for chloride efflux, is simultaneously downregulated [14][15]. This dual dysregulation creates a vicious cycle where GABA-ergic transmission shifts from inhibitory to excitatory, fundamentally undermining the mechanism of action of BZDs.

Furosemide, a loop diuretic traditionally used for cardiovascular conditions, has demonstrated unexpected anticonvulsant properties through its antagonism of NKCC1 at micromolar concentrations. Unlike conventional antiepileptic drugs that directly target neurotransmitter systems, furosemide addresses the fundamental chloride homeostasis disruption that underlies treatment resistance. Previous studies have shown furosemide's effectiveness against PTZ-induced seizures [4], but these investigations have primarily examined furosemide as a monotherapy without addressing the critical clinical challenge of BZD resistance in prolonged seizures.

The present study advances beyond prior research by systematically investigating the combination of furosemide and diazepam for seizure control. While furosemide's anticonvulsant properties have been previously documented, this work is the first to characterize its potential interaction with first-line BZD therapy in established seizure activity. This addresses an important clinical gap, as most SE patients have already received BZD treatment before alternative therapies are considered. The study employs an integrated approach combining molecular docking studies to elucidate furosemide's binding interactions with NKCC1, followed by *in vivo* validation of the combination therapy in PTZ-induced seizure models. This dual methodology provides mechanistic insight into how NKCC1 antagonism restores the efficacy of GABA-ergic modulation when chloride homeostasis is compromised. The primary purpose of this work was to investigate furosemide's capacity to enhance GABA receptor activity through NKCC1 antagonism and evaluate its therapeutic potential in combination with diazepam, thereby establishing a foundation for rational combination therapy strategies that could address the substantial unmet

clinical need in pharmaco-resistant status epilepticus.

2. MATERIALS AND METHODS

2.1. Materials

The experimental compounds utilized in this study included furosemide (Ethica Pharmaceuticals, Indonesia), diazepam as Valisanbe® (Sanbe Pharmaceuticals, Indonesia), and PTZ (GLPBIO Technology, Montclair, USA, catalog GC12357). Biochemical analysis was conducted using ELISA kits for albumin, superoxide dismutase, glutamate dehydrogenase, and interleukin-6 obtained from ELAB Science (Wuhan, China), while $GABA_A$ receptor expression was assessed using a primary monoclonal rat antibody to receptor GABAα1-6 from Santa Cruz Biotechnology Europe (catalog sc-376282). Protein extraction utilized PRO-PREP™ protease inhibitor from Intron Biotechnology Inc. (Korea, catalog 17081). All experimental compounds were dissolved in physiological saline (0.9% NaCl) to ensure consistent preparation. For in silico study, a dedicated workstation running Ubuntu 20.04 LTS was used. The system featured an Intel® Core™ i9-12900KF processor (24 CPU at 3.6 GHz), 32 GB of RAM, and an NVIDIA RTX 4060 GPU with 16 GB VRAM. Autodock 4.2 assisted with Autodock Tools interface was utilized as the molecular docking software.

2.2. Methods

2.2.1. Molecular Docking Study

Molecular docking investigations were executed using AutoDock 4.2 software with AutoDock Tools interface [16], targeting NKCC1 as the primary protein of interest. The crystallographic structure of human NKCC1 was retrieved from the Protein Data Bank (PDB ID: 7S1X) [17]. Although the *in vivo* experiments were conducted in Wistar rats, human and rat NKCC1 share high sequence homology (>95%), with full conservation of key residues in the ligand-binding site, justifying the use of the human structure as a valid model. Three-dimensional molecular structures of furosemide and diazepam were obtained from the PubChem database (CIDs 3440 and 3016, respectively).

Structural preparation of the NKCC1 protein was performed using Biovia Discovery Studio Visualizer software, incorporating comprehensive cleaning procedures that eliminated water molecules, co-crystallized ligands, heteroatoms, and non-essential protein chains to optimize the binding site for subsequent docking calculations. The furosemide and diazepam structures underwent energy minimization through molecular mechanics (MM) simulations executed in Avogadro software, employing Merck's MMFF94s force field with steepest descent optimization algorithms to achieve thermodynamically stable conformations.

The molecular docking protocol initiated with rigorous validation procedures through re-docking of the native NKCC1 ligand. Active site coordinates were defined at x: 114.02, y: 111.063, and z: 147.634, with grid-box dimensions maintained at 40 × 40 × 40 Angstroms to encompass the complete native ligand binding region. Docking calculations utilized genetic algorithm set at 100 runs and Lamarckian genetic algorithm (LGA) was used for the conformational search. Protocol validation was confirmed by achieving root-mean-square deviation (RMSD) values below 2 Å during re-docking procedures.

These validated parameters were subsequently applied to individual docking studies of furosemide and diazepam compounds, followed by comprehensive evaluation of combination models incorporating both therapeutic agents simultaneously. The development of combination docking models adhered to established methodologies [18][19]. The multi-docking procedure was executed by incorporating the ligand structure obtained from initial single-compound docking into the NKCC1 crystallographic framework using Biovia Discovery Studio software. Following the initial docking simulation, the resulting ligand-NKCC1 complex structure was preserved in PDB file format. Two distinct ligand-bound NKCC1 configurations were generated through this process, specifically the furosemide-NKCC1 complex and the diazepam-NKCC1 complex. Subsequently, molecular docking simulations were performed to evaluate diazepam binding to the furosemide-NKCC1 structure and furosemide binding to the diazepam-NKCC1 structure. These secondary docking procedures utilized identical computational parameters and

targeted the same active site coordinates that were established during the initial single-compound docking protocol.

2.2.2. In Vivo Study

2.2.2.1 Animals

This investigation employed male Wistar rats (n = 24) aged 8–9 weeks with body weights ranging from 180–240 g, sourced from the Animal House of the Food Security and Agriculture Office, Bandung City Government. The experimental procedures were conducted at Brawijaya University, Malang, Indonesia, with animal handling managed by the Integrated Research and Testing Laboratory. Prior to experimental initiation, all animals underwent a one-week acclimatization period housed in standard polycarbonate cages measuring 38 cm × 23 cm × 10 cm, with 6 animals per cage under strictly controlled environmental conditions. The housing environment maintained a 12-hour light-dark cycle with illumination from 7:00 a.m. to 7:00 p.m., ambient temperature of 22–23°C ± 2°C, and relative humidity ranging from 50–70%. Animals received ad libitum access to water and a standard laboratory diet (Pars animal food, Indonesia) containing 49.8% carbohydrates, 16% protein, 7% fat, essential minerals, vitamins, and amino acids throughout the experimental period. Following simple randomization procedures, rats were allocated to distinct experimental groups of six animals each, with each subject utilized only once during the investigation to ensure experimental integrity (Figure 1). All experimental protocols and animal care procedures adhered to established ethical standards and received formal approval from the Health Research Ethics Committee, Faculty of Medicine, Brawijaya University, Malang, Indonesia (approval number 285/EC/KEPK-83/09/2023), ensuring compliance with institutional guidelines for animal welfare and research conduct.

2.2.2.2. Seizures Rat Model Induction

The development of a status epilepticus animal model required the systematic determination of PTZ dosage necessary to reliably induce seizures of

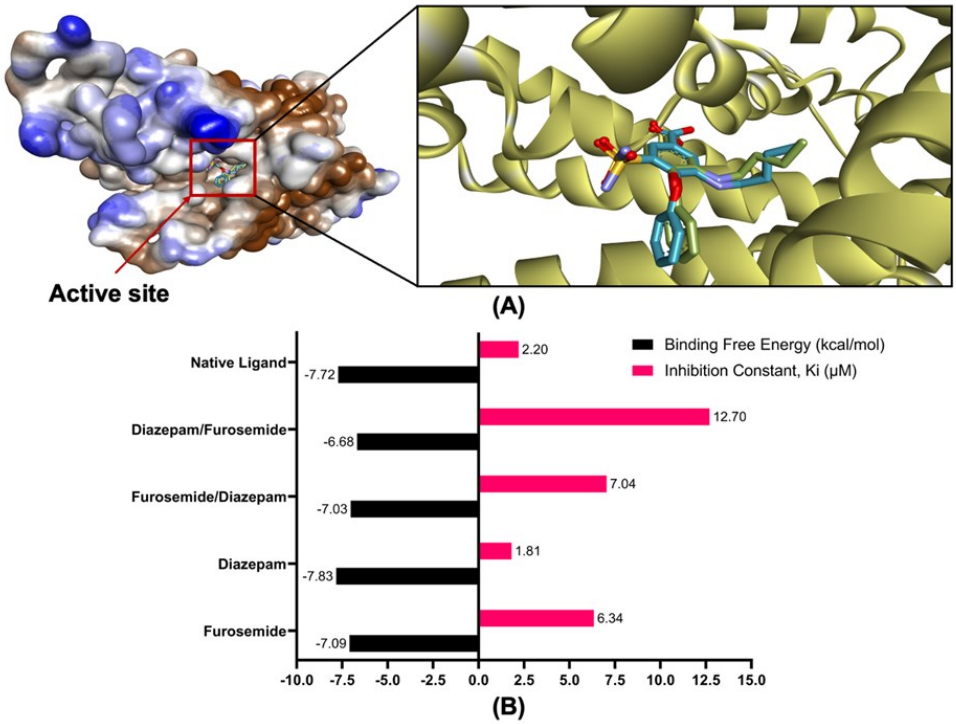

Figure 2. Molecular docking results. (A) Validation of the docking protocol with RMSD value of 0.93 Å (blue: original ligand; green: re-docked ligand), (B) Docking score.

Note: Diazepam/Furosemide" indicates the binding score of diazepam when docked into NKCC1 in the presence of furosemide, and "Furosemide/Diazepam" indicates the binding score of furosemide when docked into NKCC1 in the presence of diazepam.

appropriate severity. Seizure intensity was evaluated according to the established Racine behavioral scale, which provides a standardized classification system ranging from normal behavior (score 0) through progressive seizure manifestations including continuous ear and facial twitching (score 1), myoclonic body jerking (score 2), clonic forelimb jerking (score 3), tonic clonic seizure (score 4), generalized tonic clonic seizure (score 5), and death (score 6). Status epilepticus was defined as achieving the most severe seizure classification on the Racine scale, specifically a generalized tonic clonic seizure corresponding to a score of 5. Through preliminary dose-response studies, a PTZ dose of 90 mg/kg was established as the optimal concentration to consistently induce status epilepticus seizures with a Racine scale score of 5.

2.2.2.3. Experimental Procedure

Following PTZ administration, the experimental subjects were systematically allocated through randomization into six distinct treatment groups, each comprising six animals. The experimental design included a control group receiving normal saline (group I), a standard treatment group receiving diazepam at 3 mg/kg (group II), and a furosemide monotherapy group receiving furosemide at 50 mg/kg (group III). The combination therapy groups consisted of diazepam 3 mg/kg with furosemide at varying doses: 25, 50, and 75 mg/kg for groups IV, V, and VI, respectively. All pharmaceutical interventions were delivered via intraperitoneal injection, with PTZ dissolved in 0.9% sodium chloride solution to ensure consistent preparation and delivery. Following treatment administration, each animal was housed individually in observation cages for continuous behavioral monitoring. Seizure activity and associated behaviors were systematically documented over a 24-h period using a HIKVISION Turbo HD 7200 series digital video recording system (model IDA-7264HQHI-M1/E, Hangzhou, China) equipped with high-definition color imaging capabilities.

2.2.2.4. Evaluation of Anticonvulsant Effect

Following treatment administration, experimental subjects were housed individually in observation cages measuring 45 × 36.5 × 14.5 cm to enable precise behavioral monitoring and prevent interference between animals. The therapeutic interventions were administered 5 min after each PTZ injection to establish a standardized treatment protocol. Seizure activity and associated behavioral manifestations were systematically documented through continuous video surveillance using a HIKVISION Turbo HD 7200 series digital recording system (model IDA-7264HQHI-M1/E, Hangzhou, China) equipped with high-definition color imaging technology. The primary observation period focused on the initial 30 min following treatment injection, during which behavioral characteristics of seizure activity were recorded throughout the complete duration of each seizure episode.

2.2.2.5. Brain Collection

Following the twenty-four-hour observation period after PTZ and treatment administration, experimental subjects underwent humane euthanasia procedures for tissue collection. The entire brain, with the exception of the hippocampus, was carefully extracted and prepared for biochemical analysis. Brain tissue specimens were processed through homogenization at 4 °C using standardized volumes of phosphate-buffered saline (pH 7.4) supplemented with protease inhibitor to preserve protein integrity during processing. The resulting homogenates underwent centrifugation at 10,000 g for 15 min at 4 °C to separate cellular components, after which the supernatant fractions were collected and stored at –80 °C to maintain sample stability until subsequent biochemical parameter assessment and immunohistochemical analysis could be performed.

2.2.2.6. Biochemical Assay

Several seizure-related parameters, including IL-6 (product No: E-EL-R0015, Elabscience Biotechnology Inc, Wuhan, China), GDH (product No: ER0991, Wuhan Fine Biotech Co, Wuhan, China), albumin (product No: E-EL-R0362, Elabscience Biotechnology Inc, Wuhan, China), and superoxide dismutase (SOD, product No: ER1347, Wuhan Fine Biotech Co, Wuhan, China), were analyzed according to established manufacturer protocols. The analysis employed spectrophotometric methodology, measuring the

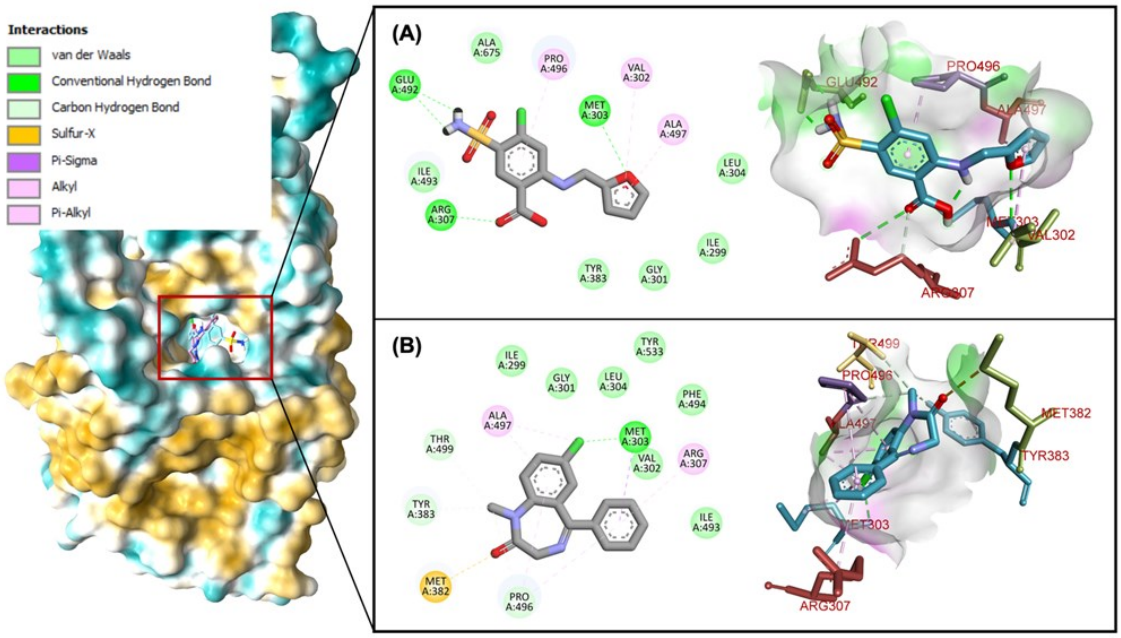

Figure 3. Molecular interactions of (A) furosemide and (B) diazepam with essential amino acid residues within NKCC1 binding pocket.

reactivity of IL-6, GDH, albumin, and SOD in chromophore formation at a wavelength of 450 nm. The concentrations of IL-6, GDH, albumin, and SOD were determined using standard calibration curves and reported in µg/mL units.

2.2.2.7. Immunohistochemistry

For histological examination, tissue specimens were procured twenty-four hours subsequent to PTZ administration and therapeutic intervention. Brain tissues were carefully extracted from the cranial cavity and systematically sectioned into 2-mm coronal segments utilizing a precision brain matrix. These specimens underwent post-fixation for twenty-four hours at 4° C in a 4% paraformaldehyde solution (PFA; Sigma-Aldrich) prepared in phosphate buffer (0.1 M Na_2HPO_4, 0.1 M NaH_2PO_4, pH 7.2). Following this procedure, tissues were transferred to phosphate-buffered saline and maintained at 4 °C for a minimum duration of forty-eight hours prior to embedding and flash-freezing in Tissue-PlusTM O.C.T. compound (Thermo Fisher Scientific, Waltham, MA). Tissue blocks were subsequently processed into 10-micrometre coronal sections through cryosectioning methodology and preserved at −80 ° C until immunohistochemical staining procedures were initiated.

The histological preparation protocol encompassed several critical stages. Initially, slides underwent baking procedures, followed by deparaffinization through two successive xylene treatments and rehydration via graduated ethanol concentrations to distilled water. Endogenous peroxidase activity was effectively eliminated through treatment with 3% hydrogen peroxide for five minutes. Antigen retrieval was accomplished by subjecting slides to heating in target retrieval solution (pH 6), succeeded by sequential rinsing with distilled water and phosphate-buffered saline. Primary antibody incubation targeting the $GABA_A\alpha_{1\text{-}6}$ receptor was conducted overnight at 4 ° C, with appropriate dilution achieved in blocking buffer. Following comprehensive PBS washing cycles, slides were processed according to stringent manufacturer protocols, incorporating streptavidin-horseradish peroxidase (SA-HRP), amplification reagent, anti-fluorescein HRP, and DAB chromogen. All immunohistochemical staining procedures were executed utilizing reagents sourced from Santa Cruz Biotechnology, Seoul, South Korea, ensuring standardized and reproducible results.

2.2.2.8. Densitometric Analysis

Immunohistochemical analysis was performed using specific antibodies targeting GABAα receptors, with quantitative assessment conducted

across three distinct neuroanatomical regions: the hippocampus, dentate gyrus, and cortical tissue. The expression levels of GABAα receptors were systematically evaluated through densitometric analysis of band intensities derived from experimental images. This quantitative analysis was executed using ImageJ software (version 1.53c, developed by Wayne Rasband, National Institutes of Health, Bethesda, MD, USA; accessible at http://imagej.nih.gov/ij), which provided standardised measurements of immunolabelling intensity. Microscopic examination and image acquisition were conducted using an Olympus BX53 microscope system (Japan) integrated with an Olympus DP72 digital camera system (Germany).

2.2.3. Statistical Analysis

Statistical analysis was performed using SPSS software version 27.0, with all data presented as means ± SD. Following assessment of normality distribution using the Shapiro-Wilk test, quantitative parameters including seizure duration, oxidative stress markers, inflammatory indicators, blood-brain barrier integrity measures, and GABAA receptor parameters were evaluated through one-way analysis of variance. To control for type I error due to multiple comparisons, appropriate post hoc tests were applied based on the comparison structure. When comparing multiple treatment groups against a single control condition, the Dunnett test was employed. For all pairwise comparisons among treatment groups, the Tukey's test was used to maintain the family-wise error rate at 0.05. Comparative analysis between two independent groups was conducted using unpaired student's t-test. The statistical significance threshold was established at $p \leq 0.05$ for all experimental comparisons, with specific correction methods indicated in the corresponding figure legends and tables.

3. RESULTS AND DISCUSSIONS

3.1. Molecular Docking Study

The assessment of furosemide's potential as an NKCC1 antagonist was conducted through systematic evaluation of its binding affinity and interaction mode with the NKCC1 active site, utilizing diazepam as a comparative standard. This evaluation employed rigorously validated computational protocols, as illustrated in Figure 2 (a), ensuring methodological reliability and reproducibility consistent with established molecular docking standards [20]. The molecular docking results reveal that furosemide demonstrates measurable binding potential with NKCC1, though its binding affinity proves inferior to that of diazepam. The quantitative analysis, presented in Figure 2(b), indicates that furosemide exhibits a less favorable free binding energy of -7.03 kcal/mol and a relatively elevated inhibition constant (Ki) of 6.34 μM compared to diazepam's superior binding parameters (free binding energy: -7.83 kcal/mol; Ki: 1.81 μM).

The investigation of combined furosemide and diazepam administration reveals antagonistic effects. The simultaneous presence of both compounds results in mutual affinity reduction, though the impact on furosemide binding remains relatively modest. Diazepam's presence minimally affects furosemide's binding parameters, evidenced by a marginal increase in free binding energy of only 0.06 kcal/mol and a Ki elevation of 0.7 μM. This minimal interference suggests potential compatibility for combination therapy approaches, consistent with pharmacological principles of drug interaction [21]. Conversely, furosemide's presence significantly compromises diazepam's binding affinity to NKCC1, resulting in substantial increases in free binding energy and Ki values of 1.15 kcal/mol and 10.89 μM, respectively. This asymmetric interaction pattern indicates competitive binding mechanisms and suggests that furosemide may interfere with diazepam's optimal therapeutic positioning within the NKCC1 active site.

The observed affinity variations result from distinct amino acid interaction patterns between furosemide and diazepam within the NKCC1 active site. Figure 3 illustrates the comprehensive molecular interactions between both compounds and specific amino acid residues within the NKCC1 binding domain. The analysis reveals that diazepam established a more extensive interaction network, forming seven distinct molecular contacts compared to furosemide's six interactions, supporting the superior binding affinity observed in quantitative measurements. Beyond interaction quantity,

diazepam demonstrated greater interaction diversity compared to furosemide. As shown in Figure 3(a), furosemide primarily established hydrogen bonding interactions with Glu 492, Arg 307, and Met 303, supplemented by alkyl interactions with Pro 496, Val 302, and Ala 497. This interaction profile, while functionally relevant, lacks the complexity observed in diazepam's binding pattern. Diazepam exhibits a more sophisticated interaction repertoire, forming hydrogen bonds with Met 303, carbon-hydrogen interactions with Thr 499 and Tyr 383, alkyl interactions with Arg 307 and Ala 497, and sulfur interactions with Met 382. This diverse interaction portfolio contributed significantly to diazepam's enhanced binding stability and superior affinity for NKCC1, consistent with structure-activity relationship principles [22][23].

The molecular docking of combination binding revealed complex interaction modifications that explain the observed affinity changes. Diazepam's presence minimally influences furosemide's NKCC1 affinity while primarily affecting its binding conformation. However, furosemide substantially impacts both diazepam's binding affinity and conformational positioning, suggesting asymmetric competitive binding mechanisms. Figure 4 illustrates the molecular interaction patterns when both compounds are administered in combination within the NKCC1 active site. The analysis demonstrates significant modifications in both interaction quantity and type for each compound, with furosemide experiencing interaction enhancement while diazepam suffers interaction reduction. In the combination scenario, furosemide maintains its original hydrogen bonding interactions with Arg 307 and Met 382, along with alkyl interactions with Pro 496. Remarkably, several novel interaction types emerge that were absent during individual administration, including halogen interactions with Glu 492, carbon-hydrogen bonding with Ile 493 and Ala 675, pi-pi T-shape interactions with Phe 682, amide-pi-stacked interactions with Ile 678, and pi-sulfur interactions with Met 382. This interaction enhancement potentially compensates for competitive binding effects, explaining furosemide's maintained affinity in combination therapy. Conversely, diazepam experiences significant interaction loss in combination, forfeiting hydrogen bonding and carbon-hydrogen interactions while retaining pi-alkyl interactions with Val 385, Cys 671, and Val 302, alongside sulfur interactions with Met 382. Notably, the number of pi-alkyl interactions increases compared to individual administration, and a novel pi-anion interaction with Glu 389 emerges. Despite these compensatory interactions, the overall binding strength reduction suggests that furosemide's presence disrupts diazepam's optimal

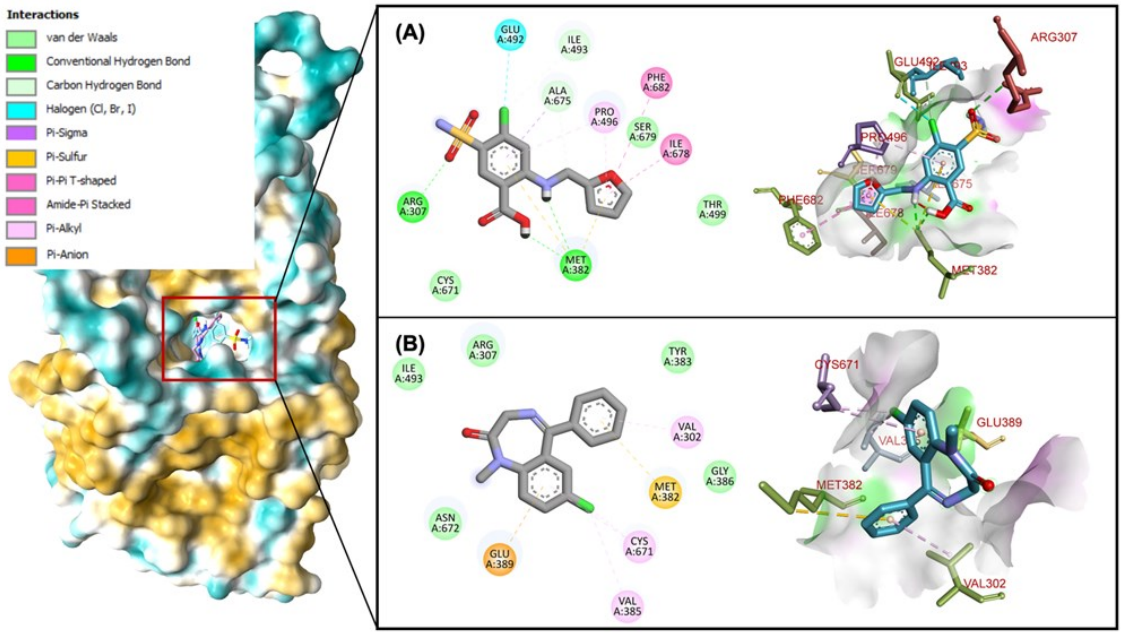

Figure 4. Molecular interaction of (A) furosemide and (B) diazepam with amino acid residues within NKCC1 binding pocket during combination phase.

binding conformation, explaining the observed affinity decrease.

These findings have significant implications for therapeutic applications of furosemide as an NKCC1 modulator. While furosemide demonstrates measurable NKCC1 binding capacity, its inferior affinity compared to established modulators suggests potential limitations in therapeutic efficacy. However, the distinct interaction profile may offer unique therapeutic advantages in specific clinical contexts, particularly where traditional NKCC1 modulators prove inadequate [24]. The combination therapy analysis reveals complex pharmacodynamic interactions that must be considered in clinical applications. The asymmetric competitive binding pattern suggests that combination protocols require careful optimization to maximize therapeutic benefits while minimizing antagonistic effects.

3.2. Effect of Furosemide on Seizure Duration and $GABA_A$ Receptor Expression In Vivo

The present study demonstrated significant anticonvulsant efficacy of furosemide both as a monotherapy and in combination with diazepam, as evidenced by two distinct neurological parameters. Regarding seizure duration (Figure 5(a)), the data reveal pronounced therapeutic benefits across all treatment modalities compared to the normal saline control group. Normal saline-treated subjects exhibited the longest seizure duration at approximately 185 ± 2.1 s, establishing the baseline pathological state. Diazepam monotherapy achieved substantial seizure reduction, decreasing duration to approximately 42.5 ± 2.1 s. Furosemide demonstrated comparable anticonvulsant activity, reducing seizure duration to approximately 77 ± 3.5 s, though this effect was moderately less pronounced than diazepam alone. The combination therapies exhibited suboptimal anticonvulsant effects, with none of the furosemide-diazepam combinations (25, 50, or 75 mg/kg) reducing seizure duration beyond the effect observed with diazepam alone. While some reductions in seizure duration were observed compared with the control, the 50 mg/kg combination did not demonstrate superior efficacy (80 ± 3.0 s), indicating that adding furosemide to diazepam does not enhance anticonvulsant activity in this model. In contrast, the seizure duration dramatically increased at diazepam-furosemide 75 mg/kg combination groups. Interestingly, statistical analysis revealed no significant difference between the furosemide and diazepam-furosemide 50 mg/kg combination groups, suggesting a potential therapeutic plateau within this dosage range. The non-linear dose-response observed—where seizure duration decreases from 25 to 50 mg/kg furosemide, then increases at 75 mg/kg when combined with diazepam—suggests complex pharmacodynamic and possibly pharmacokinetic interactions. Furosemide, a loop diuretic, has demonstrated anticonvulsant effects in animal models, particularly against chemically induced seizures (e.g., leptazol) [4]. Its mechanism is thought to involve inhibition of neuronal chloride transporters, reducing hyperexcitability. In this study, 25 and 50 mg/kg furosemide both reduced seizure severity, but only 50 mg/kg provided 100% protection at 30 min, indicating a threshold effect rather than a linear dose-response. At 50 mg/kg, furosemide may reach a concentration that interferes with optimal GABA-ergic modulation or causes paradoxical excitation, temporarily reducing efficacy before higher doses restore balance. While no direct evidence points to acute toxicity at 50 mg/kg, high doses of furosemide can cause electrolyte imbalances (e.g., hypokalemia), which may transiently increase neuronal excitability and seizure duration before compensatory mechanisms or further dose escalation counteract this effect [4].

Examination of $GABA_A$ receptor expression (Figure 5(b)) provides mechanistic insight into the observed anticonvulsant effects. Normal saline treatment resulted in the lowest receptor expression at approximately 24 ± 2.50%, consistent with seizure-induced neuronal dysfunction. Diazepam treatment significantly elevated receptor expression to approximately 41.5 ± 1.6%, reflecting its established GABA-ergic mechanism of action. Furosemide monotherapy increased receptor expression to approximately 29.8 ± 1.6%, indicating moderate enhancement of GABA-ergic neurotransmission. The combination treatments demonstrated variable effects on receptor expression, with the 25 mg/kg combination achieving the highest expression levels at approximately 37.60 ± 2.0%. The 50 mg/kg and 75

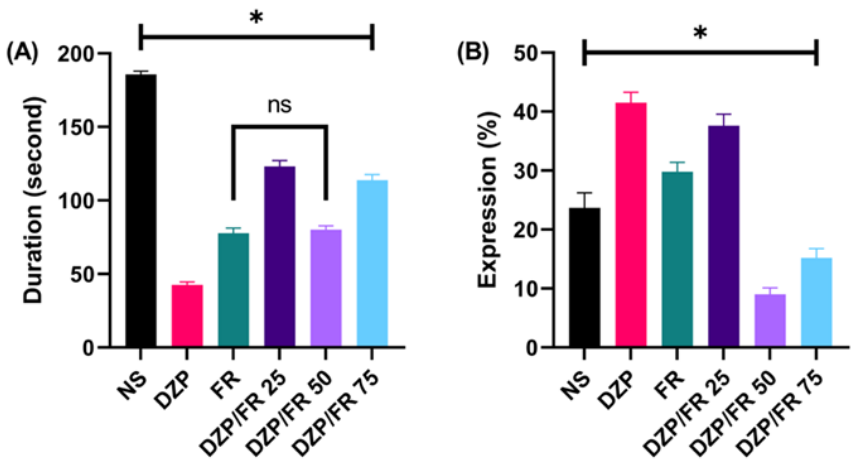

Figure 5. Anticonvulsant effect of furosemide and its combination with diazepam. (A) Duration seizures; (B) GABAA receptor expression. Data are presented as mean ± SD (n=6) and statistically analyzed using One Way ANOVA, Tukey's test. ns: not significant different ($p > 0.05$); *: significant different ($p<0.05$). NS: Normal Saline; DZP: Diazepam; FR: Furosemide.

mg/kg combinations showed progressively diminished receptor expression at approximately 9 ± 1.50% and 15.20 ± 1.65%, respectively, suggesting potential dose-dependent modulation of GABA-ergic signaling pathways.

This enhancement demonstrates furosemide's ability to restore inhibitory receptor availability through restoration of proper chloride homeostasis. The molecular basis for furosemide's therapeutic efficacy lies in its inhibition of NKCC1, which prevents the pathological accumulation of intracellular chloride that renders $GABA_A$ receptor activation excitatory rather than inhibitory during seizure states [25][26]. By maintaining appropriate chloride gradients, furosemide creates cellular conditions that permit effective GABA-ergic inhibition, thereby addressing a fundamental ionic dysfunction underlying seizure susceptibility. The dose-dependent relationship of furosemide's therapeutic effects becomes apparent when comparing the two combination therapies. Combination therapy 1 (furosemide 25 mg/kg) demonstrated superior $GABA_A$ receptor expression enhancement compared to combination therapy 2 (furosemide 50 mg/kg), despite the latter achieving better seizure duration control. This finding suggests that furosemide exhibits complex pharmacodynamics with distinct optimal dosing windows for different therapeutic endpoints. The lower furosemide dose appears more effective for receptor expression upregulation, whilst higher concentrations provide superior acute seizure control. This biphasic response pattern indicates that furosemide's therapeutic mechanisms involve multiple molecular targets beyond NKCC1 inhibition, potentially including effects on cellular metabolism and membrane stability at higher concentrations.

The molecular docking studies provide crucial validation of furosemide's therapeutic mechanisms by confirming its binding capacity to NKCC1. The computational analysis revealed that furosemide demonstrates measurable binding affinity to NKCC1 with a binding energy of -7.03 kcal/mol and a Ki of 6.34 μM, establishing its potential as a selective NKCC1 antagonist. These binding parameters confirm furosemide's capacity for direct molecular interaction with its primary therapeutic target, supporting the mechanistic rationale for its anticonvulsant properties. The competitive binding analysis demonstrates that furosemide maintains stable binding affinity to NKCC1 even in the presence of diazepam (binding energy change: +0.06 kcal/mol; Ki increase: 0.7 μM), indicating minimal competitive interference and suggesting that furosemide can maintain its therapeutic efficacy in combination protocols. Conversely, the presence of furosemide significantly compromises diazepam's binding characteristics, causing a substantial decrease in diazepam's binding affinity

(binding energy increase: +1.15 kcal/mol; Ki increase: 10.89 μM). This asymmetric interaction pattern indicates that while furosemide's binding profile remains relatively stable during co-administration, diazepam experiences a marked reduction in its molecular binding capacity. These findings suggest that the two drugs interact in a competitive manner at the NKCC1 site, and that furosemide contributes selectively to certain mechanistic domains rather than exerting a dominant therapeutic effect in the combination.

The preservation of furosemide's NKCC1 binding capacity in combination therapy provides molecular justification for the observed therapeutic synergism, whilst simultaneously revealing the compromised efficacy of diazepam in combined protocols. Unlike diazepam, which experiences significant binding affinity reduction in the presence of furosemide, furosemide maintains consistent molecular interactions with its target protein. This differential stability pattern suggests that combination therapy protocols may achieve their therapeutic benefits primarily through furosemide's maintained NKCC1 inhibitory activity rather than through genuine additive enhancement of both drugs. The marked reduction in diazepam's binding capacity (Ki increase from 1.81 to 12.70 μM) indicates that traditional benzodiazepine-mediated GABA-ergic enhancement becomes substantially attenuated when furosemide is present, positioning furosemide as the predominant therapeutic agent in combination formulations. The restoration of chloride homeostasis through furosemide's mechanism addresses the ionic basis of seizure susceptibility whilst simultaneously creating conditions that may actually impair traditional benzodiazepine-mediated therapeutic mechanisms [27]. The substantial reduction in diazepam's binding affinity when co-administered with furosemide suggests that combination therapy outcomes reflect furosemide's therapeutic dominance rather than true drug synergism. This finding has important implications for combination therapy design, as it indicates that the apparent benefits of combined protocols may arise primarily from furosemide's-maintained efficacy rather than from complementary enhancement of both therapeutic pathways. The compromised diazepam activity in combination settings may explain why higher furosemide concentrations are required to achieve optimal therapeutic outcomes, as the combination must rely predominantly on NKCC1 inhibition mechanisms.

3.3. Effect of Furosemide on Seizure Biomarkers

The PTZ-induced kindling model revealed several critical neurobiological alterations that illuminate the therapeutic mechanisms underlying different treatment approaches, as illustrated in Figure 6. PTZ-induced kindling precipitated marked neuroinflammatory changes, as reflected by elevated IL-6 concentrations. Control animals exhibited high IL-6 levels (392.60 ± 3.60 pg/mL), confirming activation of a robust inflammatory cascade following repeated seizure episodes. Diazepam monotherapy produced a modest reduction in IL-6 (357.40 ± 3.45 pg/mL), consistent with its limited anti-inflammatory capacity. Combination therapy 2 also reduced IL-6 (384.00 ± 3.0 pg/mL), although to a lesser extent than diazepam. These findings align with established evidence that seizure activity triggers microglial activation and cytokine release within the CNS [28]-[31]. The relatively weaker IL-6 reduction in the combination group suggests that furosemide's therapeutic actions may operate through mechanisms other than direct inflammatory modulation—most likely via chloride transport regulation [32] — thereby clarifying its position within the broader mechanistic framework.

The excitotoxic profile further strengthens this mechanistic interpretation. Significant alterations in GDH levels ($p = 0.031$) confirm excitotoxic stress in control animals (0.88 ± 1.21 ng/mL). Combination therapy 2 reduced GDH activity to 0.84 ± 1.65 ng/mL, indicating partial protection against excitotoxic damage. As GDH is a sensitive marker of neuronal metabolic stress [33][34], its attenuation in the combination group supports the hypothesis that diazepam–furosemide co-administration enhances cellular resilience to excitotoxic injury. Because excitotoxicity represents a core mechanism of seizure-related neuronal damage [35][36], these GDH findings integrate meaningfully with the broader therapeutic narrative.

Blood–brain barrier (BBB) integrity provided another mechanistic dimension. Elevated albumin

extravasation in control animals (98.40 ± 3.10 µg/mL) indicated substantial barrier disruption. Diazepam modestly improved BBB integrity (92.30 ± 3.00 µg/mL), while combination therapy 2 achieved the greatest protection, reducing albumin to 90.90 ± 2.70 µg/mL—more effectively than combination therapy 1 (95.70 ± 3.90 µg/mL). These findings, consistent with prior reports linking seizure activity to BBB dysfunction [37][38], highlight that the combined actions of diazepam and furosemide confer distinct vascular protective benefits. Because BBB integrity directly influences seizure severity and CNS drug distribution [37][39][40], these biomarker findings represent one of the clearest mechanistic advantages of the combination strategy.

In contrast, oxidative stress markers showed minimal contribution to the therapeutic mechanism. SOD activity did not differ significantly across groups ($p > 0.05$), with values remaining close (control: 7.08 ± 1.98 ng/mL; diazepam: 6.97 ± 2.24 ng/mL; combination therapy 2: 7.12 ± 3.01 ng/mL). These non-significant changes suggest that oxidative stress modulation likely represents a secondary rather than primary mechanism of action for either drug, consistent with prior literature indicating that oxidative effects may occur downstream of seizure activity rather than serving as the principal therapeutic target [41]-[44].

Taken together, these biomarker findings collectively clarify the mechanistic landscape of the tested therapies. Optimal therapeutic outcomes are typically characterized by decreased inflammatory burden, reduced excitotoxicity, improved BBB integrity, enhanced antioxidant function, and strengthened GABA-ergic signaling. In the present investigation, combination therapy did not outperform diazepam across all domains—particularly regarding seizure duration, IL-6 modulation, excitotoxicity, and oxidative status.

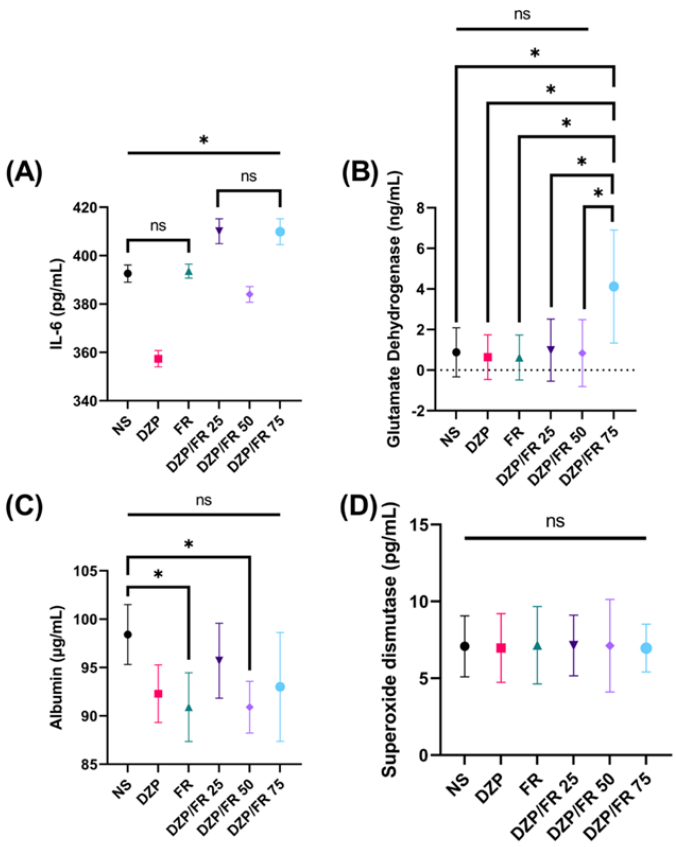

Figure 6. Effect of furosemide supplementation on biomarkers of seizures rat model. (A) IL-6, (B) glutamate dehydrogenase, (C) albumin, and (D) superoxide dismutase. Data are presented as mean ± SD (n=6) and statistically analyzed using One Way ANOVA, Tukey's test. ns: not significant different ($p>0.05$); *: significant different ($p<0.05$). NS: Normal Saline; DZP: Diazepam; FR: Furosemide.

However, combination therapy 1 did show clear mechanistic benefit in preserving BBB integrity, highlighting selective neuroprotective potential despite the absence of global superiority.

The apparent discrepancy between improvements in specific biomarkers and the lack of overall enhancement in seizure control reinforces the multifactorial nature of seizure pathophysiology. As noted in prior studies [45]-[47], isolated biomarker changes may not directly translate into comprehensive therapeutic benefit. Nevertheless, the selective BBB protection observed with combination therapy 1 underscores that different drug combinations may preferentially target distinct mechanistic pathways. Such selectivity has important implications for personalized seizure management, suggesting that combination regimens can be tailored to address individual pathophysiological vulnerabilities [48]. The clinical implications of these findings extend beyond the immediate therapeutic context. The demonstration that combination approaches can provide selective neuroprotective benefits, particularly in blood-brain barrier preservation, suggests potential applications in preventing long-term neurological sequelae of seizure disorders. Furthermore, the dose-dependent variations observed between combination therapies indicate the critical importance of optimizing drug ratios to achieve maximum therapeutic benefit while minimizing potential adverse effects, as emphasized in recent pharmacological reviews.

3.4. Effect of Furosemide on Immunohistochemistry of Seizures Rat Model Brain

The histological analysis of $GABA_A$ receptor expression in the hippocampus reveals distinct morphological characteristics across different treatment modalities in the PTZ-induced seizure model. The immunohistochemical staining, Illustrated in Figure 7, demonstrates varying degrees of receptor density and cellular distribution patterns that correspond to the therapeutic efficacy of each intervention. The control group (Figure 7 (a)) exhibits moderate $GABA_A$ receptor immunoreactivity distributed throughout the hippocampal parenchyma. The staining pattern reveals scattered positive cells with relatively uniform distribution, though the overall receptor density appears suboptimal compared to treated specimens. The cellular morphology shows typical pyramidal neuron architecture with moderately intense cytoplasmic staining, indicating baseline receptor expression levels in the seizure-induced pathological state.

Diazepam monotherapy at 3 mg/kg (Figure 7(b)) demonstrates enhanced $GABA_A$ receptor expression compared to controls. The immunohistochemical preparation reveals increased staining intensity with more pronounced receptor localization in neuronal cell bodies and dendritic processes. The distribution pattern shows improved receptor clustering, particularly in the CA1 and CA3 regions of the hippocampus, consistent with diazepam's established mechanism of enhancing GABA-ergic neurotransmission through positive allosteric modulation. Furosemide treatment at 50 mg/kg (Figure 7(c)) presents a distinctive staining profile characterized by moderate to strong immunoreactivity. The receptor expression appears more concentrated in specific neuronal populations, with enhanced perineuronal staining patterns. The morphological features suggest that furosemide induces receptor upregulation through mechanisms distinct from traditional benzodiazepine pathways, potentially involving chloride transport modulation that indirectly influences GABA-ergic signaling. The combination therapy with diazepam 3 mg/kg plus furosemide 25 mg/kg (Figure 7(d)) reveals combined effects on receptor expression. The histological examination shows intensified immunoreactivity with improved spatial distribution throughout the hippocampal architecture. The staining pattern demonstrates enhanced receptor density in both somatic and dendritic compartments, suggesting complementary mechanisms of action between the two therapeutic agents.

In marked contrast, the combination of diazepam 3 mg/kg with furosemide 50 mg/kg (Figure 7(e)) produced the most striking finding which substantially reduced GABAA receptor immunoreactivity that fell below levels observed in all other treatment groups, including monotherapies. The weak staining intensity, sparse receptor localization, and diminished overall immunoreactivity suggest that this particular dose combination may trigger counterproductive

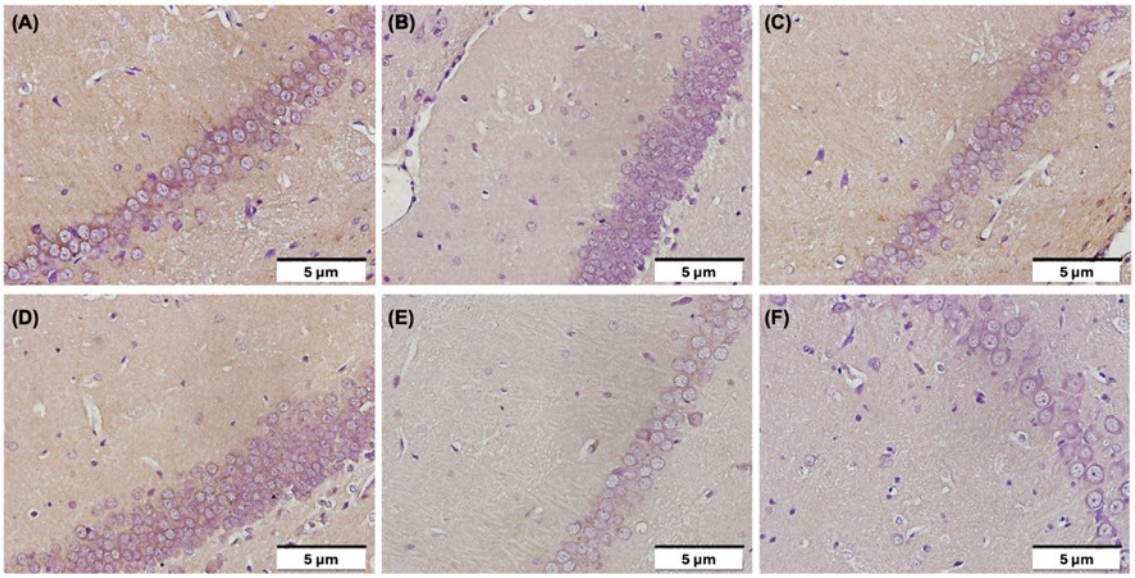

Figure 7. Immunohistochemical analysis of $GABA_A$ receptors in the rat brain (magnification of 100x). (A) Normal saline; (B) Diazepam 3 mg/kg; (C) Furosemide 50 mg/kg; (D) Diazepam 3 mg/kg + furosemide 25 mg/kg; (E) Diazepam 3 mg/kg + furosemide 50 mg/kg; (F) Diazepam 3 mg/kg + furosemide 75 mg/kg.

molecular interactions. Potential mechanisms underlying this unexpected suppression include excessive perturbation of chloride gradients leading to compensatory receptor internalization, competitive interference with receptor trafficking pathways, or induction of adaptive downregulation in response to perceived excessive GABA-ergic tone. This paradoxical reduction in receptor expression provides a plausible molecular explanation for the prolonged seizure durations observed with combination therapies in the behavioral data.

The highest dose combination of diazepam 3 mg/kg with furosemide 75 mg/kg (Figure 7(f)) demonstrated partial recovery of receptor expression relative to the 50 mg/kg combination, though immunoreactivity remained suboptimal compared to lower-dose combinations and monotherapies. The moderate staining intensity with heterogeneous distribution patterns suggests incomplete restoration of receptor homeostasis, potentially reflecting dose-dependent biphasic effects wherein intermediate furosemide doses maximally disrupt receptor regulation while higher doses engage compensatory mechanisms that partially mitigate these effects. Alternatively, the uneven distribution may indicate regional variability in sensitivity to combination therapy, with certain hippocampal subfields maintaining receptor expression while others experience sustained downregulation. The comparative histological analysis reveals that combination therapies generally enhance $GABA_A$ receptor expression beyond what is achieved with monotherapy approaches. The optimal receptor upregulation occurs with the intermediate combination dose, while higher concentrations may paradoxically reduce therapeutic efficacy. These morphological findings provide crucial insights into the dose-dependent relationship between drug combinations and receptor expression patterns in seizure management protocols.

4. CONCLUSIONS

This study provides a preclinical evaluation of the molecular interactions and mechanistic effects associated with diazepam, furosemide, and their combination within the PTZ-kindling model. Our findings indicate that furosemide exhibits measurable NKCC1 binding capacity, albeit with lower affinity than diazepam, and that combination therapy produces complex binding dynamics that influence receptor interactions and downstream biomarker profiles. These results suggest that diazepam and furosemide may exert complementary mechanistic effects, through modulation of NKCC1 activity, GABA-ergic

signaling, and selected neuroinflammatory and excitotoxic pathways, within the context of seizure-related pathophysiology. However, the present investigation is exploratory and preclinical in nature, and the observed molecular and biomarker changes should not be interpreted as direct evidence of clinical efficacy. Instead, these findings provide foundational mechanistic insights that may guide future hypothesis-driven research. Additional studies, including advanced in vivo experiments, pharmacodynamic modeling, and structural optimization of NKCC1-targeting compounds, are required before determining whether the diazepam–furosemide combination holds any translational relevance. Ultimately, this work contributes to a growing body of evidence supporting further investigation of NKCC1 modulation as a potential complementary strategy in seizure research.

AUTHOR INFORMATION

Corresponding Author

Marsintauli Hasudungan Siregar — Doctoral Program in Medical Science, Brawijaya University, Malang-65145 (Indonesia);
orcid.org/0009-0003-5377-9062
Email: marsintauli@student.ub.ac.id

Authors

Nurdiana Nurdiana — School of Pharmacy, Brawijaya University, Malang-65145 (Indonesia);
orcid.org/0000-0002-7953-1124

Farhad Bal'afif — Department of Neurosurgery, Brawijaya University, Malang-65145 (Indonesia); Saiful Anwar Hospital, Malang- 65112 (Indonesia);
orcid.org/0000-0001-8801-3719

Susanthy Djajalaksana — Saiful Anwar Hospital, Malang- 65112 (Indonesia); Department of Pulmonology and Respiratory Medicine, Brawijaya University, Malang-65145 (Indonesia);
orcid.org/0000-0002-2069-7357

Arif Setiawansyah — Pharmacy Diploma Program, Akademi Farmasi Cendikia Farma Husada, Bandar Lampung-35134 (Indonesia);
orcid.org/0000-0002-1443-8666

Author Contributions

Conceptualization, Formal Analysis, Data Curation, Project Administration, and Funding Acquisition, M. H. S.; Methodology, Validation, Investigation, Resources, and Writing – Original Draft Preparation, M. H. S. and A. S.; Software, and Visualization, A. S.; Writing – Review & Editing, M. H. S., N. N., F. B., S. D. and A. S.; Supervision, N. N., F. B., and S. D.

Conflicts of Interest

The authors declare no conflict of interest.

ACKNOWLEDGEMENT

This research receives no external funding. Authors would like to acknowledge the Faculty of Medicine, Universitas Brawijaya for the laboratory support and Akademi Farmasi Cendikia Farma Husada for the High-Performance Computing support.

DECLARATION OF GENERATIVE AI

This study used artificial intelligence (AI) tool of which AI-based language model Grammarly was employed in the language refinement (improving grammar, sentence structure, and readability of the manuscript). We confirm that all AI-assisted processes were critically reviewed by the authors to ensure the integrity and reliability of the results. The final decisions and interpretations presented in this article were solely made by the authors.

REFERENCES

[1] S. Sivakumaran and J. Maguire. (2016). "Bumetanide Reduces Seizure Progression And The Development Of Pharmacoresistant Status Epilepticus". *Epilepsia.* **57** (2): 222-232. 10.1111/epi.13270.

[2] E. Sallard, D. Letourneur, and P. Legendre. (2021). "Electrophysiology Of Ionotropic GABA Receptors". *Cellular and Molecular Life Sciences.* **78** (13): 5341-5370. 10.1007/s00018-021-03846-2.

[3] S. B. Sarasa, R. Mahendran, G. Muthusamy, B. Thankappan, D. R. F. Selta, and J. Angayarkanni. (2020). "A Brief Review On

The Non-Protein Amino Acid, Gamma-Amino Butyric Acid (GABA): Its Production And Role In Microbes". *Current Microbiology.* **77** (4): 534-544. 10.1007/s00284-019-01839-w.

[4] S. E. Oriaifo, I. Otokiti, and E. K. Omogbai. (2012). "The Effect Of Furosemide On Experimentally-Induced Seizures In Mice". *Journal of Clinical Medicine and Research.* **4** (7): 89-93. 10.5897/JCMR12.003.

[5] D. E. Naylor. (2023). "In The Fast Lane: Receptor Trafficking During Status Epilepticus". *Epilepsia Open.* **8** (S1): S35-S65. 10.1002/epi4.12718.

[6] T. Z. Deeb, J. Maguire, and S. J. Moss. (2012). "Possible Alterations In GABAA Receptor Signaling That Underlie Benzodiazepine-Resistant Seizures". *Epilepsia.* **53** (S9): 79-88. 10.1111/epi.12037.

[7] M. Charalambous, H. A. Volk, L. Van Ham, and S. F. M. Bhatti. (2021). "First-Line Management Of Canine Status Epilepticus At Home And In Hospital: Opportunities And Limitations Of The Various Administration Routes Of Benzodiazepines". *BMC Veterinary Research.* **17** (1): 103. 10.1186/s12917-021-02805-0.

[8] C. H. Vinkers and B. Olivier. (2012). "Mechanisms Underlying Tolerance After Long-Term Benzodiazepine Use: A Future For Subtype-Selective GABAA Receptor Modulators". *Advances in Pharmacological and Pharmaceutical Sciences.* **2012** : 416864. 10.1155/2012/416864.

[9] P. M. Abruzzo, C. Panisi, and M. Marini. (2021). "The Alteration Of Chloride Homeostasis GABAergic Signaling In Brain Disorders: Could Oxidative Stress Play A Role". *Antioxidants.* **10** (8): 1316. 10.3390/antiox10081316.

[10] J. T. Schulte, C. J. Wierenga, and H. Bruining. (2018). "Chloride Transporters And GABA Polarity In Developmental Neurological And Psychiatric Conditions". *Neuroscience and Biobehavioral Reviews.* **90** : 260-271. 10.1016/j.neubiorev.2018.05.001.

[11] M. Hamze, C. Brier, E. Buhler, J. Zhang, I. Medina, and C. Porcher. (2024). "Regulation Of Neuronal Chloride Homeostasis By Pro And Mature Brain Derived Neurotrophic Factor BDNF Via KCC2 Cation Chloride Cotransporters In Rat Cortical Neurons". *International Journal of Molecular Sciences.* **25** (11): 6253. 10.3390/ijms25116253.

[12] R. F. Berman. (2009). In: " P. A. Schwartzkroin (Ed.) Encyclopedia of Basic Epilepsy Research". Academic Press. 10.1016/B978-012373961-2.00270-8.

[13] R. J. Burman, J. S. Selfe, J. H. Lee, M. Van Den Berg, A. Calin, N. K. Codadu, R. Wright, S. E. Newey, R. R. Parrish, A. A. Katz, J. M. Wilmshurst, C. J. Akerman, A. J. Trevelyan, and J. V. Raimondo. (2019). "Excitatory GABAergic Signalling Is Associated With Benzodiazepine Resistance In Status Epilepticus". *Brain.* **142** (11): 3482-3501. 10.1093/brain/awz283.

[14] R. Liu, J. Wang, S. Liang, G. Zhang, and X. Yang. (2020). "Role Of NKCC1 And KCC2 In Epilepsy: From Expression To Function". *Frontiers in Neurology.* **10** : 1407. 10.3389/fneur.2019.01407.

[15] Z. Talifu, Y. Pan, H. Gong, X. Xu, C. Zhang, D. Yang, F. Gao, Y. Yu, L. Du, and J. Li. (2022). "The Role Of KCC2 And NKCC1 In Spinal Cord Injury: From Physiology To Pathology". *Frontiers in Physiology.* **13** : 1045520. 10.3389/fphys.2022.1045520.

[16] G. M. Morris, R. Huey, W. Lindstrom, M. F. Sanner, R. K. Belew, D. S. Goodsell, and A. J. Olson. (2009). "AutoDock4 And AutoDockTools4: Automated Docking With Selective Receptor Flexibility". *Journal of Computational Chemistry.* **30** (16): 2785-2791. 10.1002/jcc.21256.

[17] Y. Zhao, K. Roy, P. Vidossich, L. Cancedda, M. De Vivo, B. Forbush, and E. Cao. (2022). "Structural Basis For Inhibition Of The Cation-Chloride Cotransporter NKCC1 By The Diuretic Drug Bumetanide". *Nature Communications.* **13** (1): 2747. 10.1038/s41467-022-30407-3.

[18] A. Setiawansyah, G. Susanti, R. Alrayan, I. Hadi, M. I. Arsul, D. Luthfiana, L. Wismayani, and N. Hidayati. (2024). "Aaptamine Enhanced Doxorubicin Activity On B-Cell Lymphoma 2 (Bcl-2): A Multi-

Structural Molecular Docking Study". *Ad-Dawaa' Journal of Pharmaceutical Science.* **7** (1): 1-10. 10.24252/djps.v7i1.46796.

[19] Y. Rosa, R. Riyanto, G. Susanti, A. Setiawansyah, Z. Zuhana, A. Fatriansari, and S. A. Pratama. (2024). "Persea Americana Leaf Extract Promotes Wound Healing By Inhibiting NF-KB1". *Journal of Applied Pharmaceutical Science.* 10.7324/JAPS.2025.218012.

[20] N. Nurhidayati, Y. Yueniwati, A. T. Endharti, H. K. Permatasari, and A. Setiawansyah. (2025). "Chemical Binding Free Energy And Anti-Free Radical Of Chemical Compounds From Sea Cucumber (Holothuria Scabra) Against Malondialdehyde And Akt". *Advanced Journal of Chemistry Section A.* 1709-1723. 10.48309/ajca.2025.518195.1827.

[21] N. Chaachouay. (2025). "Synergy, Additive Effects, And Antagonism Of Drugs With Plant Bioactive Compounds". *Drugs and Drug Candidates.* **4** (1): 4. 10.3390/ddc4010004.

[22] M. Lakshmanan. (2019). In: " G. M. Raj and R. Raveendran (Eds.) Introduction To Basics Of Pharmacology And Toxicology: General And Molecular Pharmacology". Springer Singapore. 10.1007/978-981-32-9779-1_13.

[23] A. Setiawansyah and B. M. Gemantari. (2022). "Potential Activity Of Caryophyllene Derivatives As Xanthine Oxidase Inhibitor: An In Silico Quantitative Structure Activity Relationship Analysis". *Journal of Food and Pharmaceutical Sciences.* **10** (3): 700-708. 10.22146/jfps.5485.

[24] Y. Ben-Ari. (2017). "NKCC1 Chloride Importer Antagonists Attenuate Many Neurological And Psychiatric Disorders". *Trends in Neurosciences.* **40** (9): 536-554. 10.1016/j.tins.2017.07.001.

[25] Y. Zhao, P. Vidossich, B. Forbush, J. Ma, J. Rinehart, M. De Vivo, and E. Cao. (2025). "Structural Basis For Human NKCC1 Inhibition By Loop Diuretic Drugs". *The EMBO Journal.* **44** (5): 1540-1562. 10.1038/s44318-025-00368-6.

[26] L. Chen, J. Yu, L. Wan, Z. Wu, G. Wang, Z. Hu, L. Ren, J. Zhou, B. Qian, X. Zhao, J. Zhang, X. Liu, and Y. Wang. (2022). "Furosemide Prevents Membrane KCC2 Downregulation During Convulsant Stimulation In The Hippocampus". *IBRO Neuroscience Reports.* **12** : 355-365. 10.1016/j.ibneur.2022.04.010.

[27] T. Z. Deeb, Y. Nakamura, G. D. Frost, P. A. Davies, and S. J. Moss. (2013). "Disrupted Chloride Homeostasis Contributes To Reductions In The Inhibitory Efficacy Of Diazepam During Hyperexcited States". *European Journal of Neuroscience.* **38** (3): 2453-2467. 10.1111/ejn.12241.

[28] Y. Chen, M. M. Nagib, N. Yasmen, M. N. Sluter, T. L. Littlejohn, Y. Yu, and J. Jiang. (2023). "Neuroinflammatory Mediators In Acquired Epilepsy: An Update". *Inflammation Research.* **72** (4): 683-701. 10.1007/s00011-023-01700-8.

[29] N. Dupuis and S. Auvin. (2015). "Inflammation And Epilepsy In The Developing Brain: Clinical And Experimental Evidence". *CNS Neuroscience and Therapeutics.* **21** (2): 141-151. 10.1111/cns.12371.

[30] M. Maroso, S. Balosso, T. Ravizza, J. Liu, E. Aronica, A. M. Iyer, C. Rossetti, M. Molteni, M. Casalgrandi, A. A. Manfredi, M. E. Bianchi, and A. Vezzani. (2010). "Toll-Like Receptor 4 And High Mobility Group Box-1 Are Involved In Ictogenesis And Can Be Targeted To Reduce Seizures". *Nature Medicine.* **16** (4): 413-419. 10.1038/nm.2127.

[31] K. Riazi, M. A. Galic, J. B. Kuzmiski, W. Ho, K. A. Sharkey, and Q. J. Pittman. (2008). "Microglial Activation And TNFα Production Mediate Altered CNS Excitability Following Peripheral Inflammation". *Proceedings of the National Academy of Sciences of the United States of America.* **105** (44): 17151-17156. 10.1073/pnas.0806682105.

[32] V. I. Dzhala, D. M. Talos, D. A. Sdrulla, A. C. Brumback, G. C. Mathews, T. A. Benke, E. Delpire, F. E. Jensen, and K. J. Staley. (2005). "NKCC1 Transporter Facilitates Seizures In The Developing Brain". *Nature Medicine.* **11** (11): 1205-1213. 10.1038/nm1301.

[33] C. Chretien, A. M. R. Lobo, A. D. La Rossa, and P. Maechler. (2023). "Glutamate Dehydrogenase Mutation Reveals The Role Of Mediobasal Hypothalamus In The Development Of Seizures". *IBRO Neuroscience Reports.* **15** : S251-S252. 10.1016/j.ibneur.2023.08.425.

[34] S. N. Rakhade and F. E. Jensen. (2009). "Epileptogenesis In The Immature Brain: Emerging Mechanisms". *Nature Reviews Neurology.* **5** (7): 380-391. 10.1038/nrneurol.2009.80.

[35] M. Barker-Haliski and H. S. White. (2015). "Glutamatergic Mechanisms Associated With Seizures And Epilepsy". *Cold Spring Harbor Perspectives in Medicine.* **5** (8): a022863. 10.1101/cshperspect.a022863.

[36] P. Ambrogini, P. Torquato, D. Bartolini, M. C. Albertini, D. Lattanzi, M. Di Palma, R. Marinelli, M. Betti, A. Minelli, R. Cuppini, and F. Galli. (2019). "Excitotoxicity, Neuroinflammation And Oxidant Stress As Molecular Bases Of Epileptogenesis And Epilepsy Derived Neurodegeneration: The Role Of Vitamin E". *Biochimica et Biophysica Acta - Molecular Basis of Disease.* **1865** (6): 1098-1112. 10.1016/j.bbadis.2019.01.026.

[37] A. Friedman, D. Kaufer, and U. Heinemann. (2009). "Blood Brain Barrier Breakdown Inducing Astrocytic Transformation: Novel Targets For The Prevention Of Epilepsy". *Epilepsy Research.* **85** : 142-149. 10.1016/j.eplepsyres.2009.03.005.

[38] N. Marchi, L. Angelov, T. Masaryk, V. Fazio, T. Granata, N. Hernandez, K. Hallene, T. Diglaw, L. Franic, I. Najm, and D. Janigro. (2007). "Seizure Promoting Effect Of Blood Brain Barrier Disruption". *Epilepsia.* **48** (4): 732-742. 10.1111/j.1528-1167.2007.00988.x.

[39] L. Han. (2021). "Modulation Of The Blood Brain Barrier For Drug Delivery To Brain". *Pharmaceutics.* **13** (12): 2024. 10.3390/pharmaceutics13122024.

[40] S. Zhang, L. Gan, F. Cao, H. Wang, P. Gong, C. Ma, L. Ren, Y. Lin, and X. Lin. (2022). "The Barrier And Interface Mechanisms Of The Brain Barrier And Brain Drug Delivery". *Brain Research Bulletin.* **190** : 69-83. 10.1016/j.brainresbull.2022.09.017.

[41] L. A. Mendez-Cuesta, B. Marquez-Valadez, V. P. La Cruz, C. Escobar-Briones, S. Galvan -Arzate, Y. Alvarez-Ruiz, P. D. Maldonado, R. A. Santana, A. Santamaria, and P. Carrillo -Mora. (2011). "Diazepam Blocks Striatal Lipid Peroxidation And Improves Stereotyped Activity In A Rat Model Of Acute Stress". *Basic and Clinical Pharmacology and Toxicology.* **109** (5): 350-356. 10.1111/j.1742-7843.2011.00738.x.

[42] S. Musavi and P. Kakkar. (2000). "Pro And Antioxidant Responses To Repeated Administration Of Diazepam In Rat Brain". *Molecular and Cellular Biochemistry.* **206** (1): 97-103. 10.1023/A:1007007630118.

[43] B. L. S. Amaral, T. P. D. Santos, R. M. D. Santos, P. F. P. Andrade, A. Rocha-Gomes, V. J. Lages, K. B. Costa, D. A. Freitas, B. F. Mendes, G. E. B. A. Melo, and W. F. Pereira. (2023). "Furosemide Reduces TNF Levels And Increases Antioxidant Activity In Animal Models Of Nephrotic Syndrome". *Journal of Advances in Medicine and Medical Research.* **35** (21): 66-79. 10.9734/jammr/2023/v35i215213.

[44] S. Kovac, A. M. Domijan, M. C. Walker, and A. Y. Abramov. (2012). "Prolonged Seizure Activity Impairs Mitochondrial Bioenergetics And Induces Cell Death". *Journal of Cell Science.* **125** (7): 1796-1806. 10.1242/jcs.099176.

[45] N. N. Wang, F. Cao, L. H. Zhang, Y. F. Zheng, and D. Xu. (2025). "Multi Omics: A Bridge Connecting Genotype And Phenotype For Epilepsy". *Biomarker Research.* 10.1186/s40364-025-00798-8.

[46] J. A. French, A. M. Kanner, J. Bautista, B. Abou-Khalil, T. Browne, C. L. Harden, W. H. Theodore, C. Bazil, J. Stern, S. C. Schachter, D. Bergen, D. Hirtz, G. D. Montouris, M. Nespeca, B. Gidal, W. J. Marks, W. R. Turk, J. H. Fischer, B. Bourgeois, A. Wilner, R. E. Faught, R. C. Sachdeo, A. Beydoun, and T. A. Glauser. (2004). "Efficacy And Tolerability Of The New Antiepileptic Drugs I: Treatment Of

New Onset Epilepsy". *Epilepsia.* **45** (5): 401-409. 10.1111/j.0013-9580.2004.06204.x.

[47] T. Granata, L. Fusco, S. Matricardi, A. Tozzo, D. Janigro, and R. Nabbout. (2022). "Inflammation In Pediatric Epilepsies: Update On Clinical Features And Treatment Options". *Epilepsy and Behavior.* **131** : 107959. 10.1016/j.yebeh.2021.107959.

[48] E. Perucca, J. French, and M. Bialer. (2007). "Development Of New Antiepileptic Drugs: Challenges Incentives And Recent Advances". *The Lancet Neurology.* **6** (9): 793-804. 10.1016/S1474-4422(07)70215-6.